

ARTICLE

Received 22 Jul 2014 | Accepted 9 Sep 2014 | Published 15 Oct 2014

DOI: 10.1038/ncomms6182

OPEN

Parkin regulates kainate receptors by interacting with the GluK2 subunit

AnnaMaria Maraschi^{1,*}, Andrea Ciammola^{1,*}, Alessandra Folci², Francesca Sassone¹, Giuseppe Ronzitti^{3,†}, Graziella Cappelletti⁴, Vincenzo Silani^{1,5}, Shigeto Sato⁶, Nobutaka Hattori⁶, Michele Mazzanti⁴, Evelina Chieregatti³, Christophe Mulle⁷, Maria Passafaro^{2,§} & Jenny Sassone^{1,†,§}

Although loss-of-function mutations in the *PARK2* gene, the gene that encodes the protein parkin, cause autosomal recessive juvenile parkinsonism, the responsible molecular mechanisms remain unclear. Evidence suggests that a loss of parkin dysregulates excitatory synapses. Here we show that parkin interacts with the kainate receptor (KAR) GluK2 subunit and regulates KAR function. Loss of parkin function in primary cultured neurons causes GluK2 protein to accumulate in the plasma membrane, potentiates KAR currents and increases KAR-dependent excitotoxicity. Expression in the mouse brain of a parkin mutant causing autosomal recessive juvenile parkinsonism results in GluK2 protein accumulation and excitotoxicity. These findings show that parkin regulates KAR function *in vitro* and *in vivo*, and suggest that KAR upregulation may have a pathogenetic role in parkin-related autosomal recessive juvenile parkinsonism.

¹IRCCS Istituto Auxologico Italiano, Department of Neurology and Laboratory of Neuroscience, Cusano Milanino, 20095 Milan, Italy. ²CNR Institute of Neuroscience, Department of BIOMETRA, University of Milan, 20129 Milan, Italy. ³Department of Neuroscience and Brain Technologies, Istituto Italiano di Tecnologia, 16163 Genova, Italy. ⁴Department of Biosciences, Università degli Studi di Milano, 20122 Milan, Italy. ⁵'Dino Ferrari' Center, Department of Pathophysiology and Transplantation, Università degli Studi di Milano, 20122 Milan, Italy. ⁶Department of Neurology, Juntendo University School of Medicine, 113-8421 Tokyo, Japan. ⁷Interdisciplinary Institute for Neuroscience, CNRS UMR 5297, University of Bordeaux, 33000 Bordeaux, France. * These authors contributed equally to this work. § These authors jointly supervised this work. † Present addresses: Genethon, Evry 91000, France (G.R.) or Neuroalgology and Headache Unit, IRCCS Foundation, 'Carlo Besta' Neurological Institute, Milan, Italy (J.S.). Correspondence and requests for materials should be addressed to J.S. (email: jenny.sassone@istituto-besta.it).

Although loss-of-function mutations in the *PARK2* gene cause the most common form of autosomal recessive juvenile parkinsonism (ARJP)^{1,2}, the underlying molecular mechanism remains unclear. The *PARK2* gene encodes the parkin protein, an ubiquitin E3 ligase widely expressed throughout the central nervous system whose functions include targeting proteins for degradation³ and modulating mitochondria turnover^{4,5}. Beside these well-recognized functions, increasing evidence suggests that parkin also regulates excitatory synapses. Immunofluorescence studies have detected widespread parkin expression in neurons, including dendrites and spines⁶. The carboxy-terminal domain of parkin contains a class II PDZ-binding motif that binds the protein CASK in postsynaptic densities⁷. Parkin associates with and ubiquitinates the PDZ protein PICK1, thus modulating the activity of ion channels involved in synaptic plasticity⁸. Parkin also mediates endophilin-A1 ubiquitination and some evidence suggests that endophilin-A-mediated parkin recruitment promotes synaptic protein ubiquitination⁹. The loss of endogenous parkin sensitizes *in vitro* midbrain dopaminergic neurons to kainate toxicity¹⁰, increases excitatory glutamatergic synapse numbers and increases vulnerability to synaptic excitotoxicity in cultured hippocampal neurons⁶. Hence, although current knowledge strongly suggests that parkin intervenes in modulating glutamatergic synapse function, the underlying molecular mechanism is unknown. We hypothesized that parkin may directly regulate ionotropic glutamate receptors of the *N*-methyl-D-aspartate (NMDAR), α -amino-3-hydroxy-5-methyl-4-isoxazolepropionic acid (AMPA) or kainate receptor (KAR) types. Our results show that parkin regulates KAR function and suggest that KAR may have a pathogenetic role in parkin-related ARJP.

Results

Increased GluK2 levels in *PARK2* brain tissues. The parkin-Q311X transgenic model expresses a human parkin variant causing ARJP¹¹, and it is the first parkin-based mouse model that exhibits a neurodegenerative phenotype *in vivo*¹². To test the hypothesis that parkin regulates glutamate ionotropic receptors, we analysed NMDAR, AMPAR and KAR subunit levels in substantia nigra from parkin-Q311X mice and littermate age-matched controls (mouse genotyping is reported in Supplementary Fig. 1a). The levels of the KAR GluK2 subunit were significantly higher in lysates from parkin-Q311X mice than from control mice (mean GluK2 values: controls 1.00 ± 0.09 versus *PARK2* 1.51 ± 0.08 , unpaired *t*-test $**P = 0.0010$), whereas the levels of AMPAR (GluA1 and GluA2/3) and NMDAR subunits (GluN1 and GluN2B) were similar in the two groups (Fig. 1a; GluK2a antibody validation is reported in Supplementary Fig. 1b; full blotting images are reported in Supplementary Fig. 2). To investigate whether GluK2 protein accumulates in ARJP patients' brains, we analysed NMDAR, AMPAR and KAR subunit levels in brain lysates from healthy controls ($n = 5$) and patients with the *PARK2* mutation ($n = 4$). Patient's data are reported in Supplementary Table. 1. GluA1 subunit levels were lower in brain lysates from patients than in those from controls (mean GluA1 values: controls 1.00 ± 0.01 versus *PARK2* 0.58 ± 0.06 , unpaired *t*-test $***P = 0.0001$; Fig. 1b). GluK2 subunit levels were markedly higher in brain lysates from patients than in those from controls (mean GluK2 values: controls 1.00 ± 0.03 versus *PARK2* 2.41 ± 0.22 , unpaired *t*-test $***P = 0.0002$; Fig. 1b; full blotting images are reported in Supplementary Fig. 3). GluK2 protein levels therefore increased in two independent *PARK2* models, the difference suggesting that parkin may interact with and regulate GluK2 protein.

Parkin interacts with the KAR GluK2 subunit. We tested the interaction hypothesis in HEK293T cells transfected with GluK2a and parkin. We found that parkin co-immunoprecipitated with GluK2a and that GluK2a co-immunoprecipitated with parkin (Fig. 2a and Supplementary Fig. 4). The co-immunoprecipitation intensities were weak but consistently above background levels. Fluorescence resonance energy transfer (FRET) experiments between GluK2a-YFP and CFP-parkin expressed in HEK293T cells indicated a direct interaction between the two proteins (Supplementary Fig. 5a). We therefore hypothesized that the parkin-GluK2 interaction might be a transient phenomenon dependent on agonist stimulation. We found that activation of GluK2 KARs with 10 mM glutamate increased parkin-GluK2a interaction in HEK293T cells as assessed by immunoprecipitation (untreated 1.00 ± 0.27 versus glutamate treated 2.70 ± 0.31 , unpaired *t*-test $**P = 0.0061$; Supplementary Fig. 5b) and FRET experiments (Supplementary Fig. 5a).

We next investigated whether the parkin-GluK2 interaction exists in brain tissues, and found that endogenous GluK2 co-immunoprecipitated with parkin in lysates from wild-type (wt) mouse brains (Fig. 2b and Supplementary Fig. 6). No co-immunoprecipitation was detected in the negative controls, that is, lysates from parkin^{-/-} and GluK2^{-/-} mouse brains (Supplementary Fig. 5c). Finally, we showed that GluK2 co-immunoprecipitated with parkin in lysates from whole human brains (Fig. 2b and Supplementary Fig. 6). The co-immunoprecipitation intensities were weak but consistently above background levels. Hence, these data show that parkin interacts with GluK2.

Many GluK2 interactors bind to the GluK2 C-terminal cytoplasmic tail, which corresponds to amino acids (aa) 841–908 in the human GluK2a isoform¹³. We therefore conducted co-immunoprecipitation experiments between parkin and GluK2a mutants with truncations of the C-terminal tail. Parkin co-immunoprecipitated with all GluK2a mutants, including the shorter GluK2a-850stop (Fig. 2c and Supplementary Fig. 6), thus suggesting that parkin binds to aa 841–850 of GluK2a. A pull-down assay using biotinylated peptides spanning the GluK2a C terminus and lysates from human brain or HEK293T cells expressing FLAG-parkin showed that parkin binds to GluK2a aa 841–850 and that parkin can also bind to a second GluK2a domain lying between aa 873 and 877 (Fig. 2d and Supplementary Fig. 7). Once we had identified the GluK2a domain responsible for parkin binding, we investigated which parkin domain mediated parkin binding to GluK2. A pull-down assay using GluK2a peptides and parkin domains showed that parkin binding specifically depends on the Ubl-linker domain (Fig. 2e and Supplementary Fig. 7). Hence, data from Fig. 2 and Supplementary Figs 4–7 show that parkin interacts directly with GluK2 and that the interaction is mediated by the Ubl-linker domain of parkin and the proximal part of the GluK2 C-terminal cytoplasmic tail. In addition, glutamate stimulation of KARs favours the parkin-GluK2 interaction.

Parkin can ubiquitinate GluK2. As parkin binding to GluK2 specifically depends on the Ubl-linker domain, which binds ubiquitination substrates¹⁴, we hypothesized that parkin could ubiquitinate GluK2. To test this possibility, we incubated purified GluK2a with HA-ubiquitin, E1, E2 (UbcH7) *in vitro*. We observed that recombinant parkin increased GluK2 ubiquitination (no parkin 1.00 ± 0.08 versus wt parkin 1.43 ± 0.14 , unpaired *t*-test $*P = 0.0201$; Fig. 3a and Supplementary Fig. 8). We confirmed that parkin-ubiquitinated GluK2a expressed in HEK293T cells transfected with Myc-GluK2a, HA-ubiquitin and parkin. Transfection of parkin significantly increased Myc-GluK2a

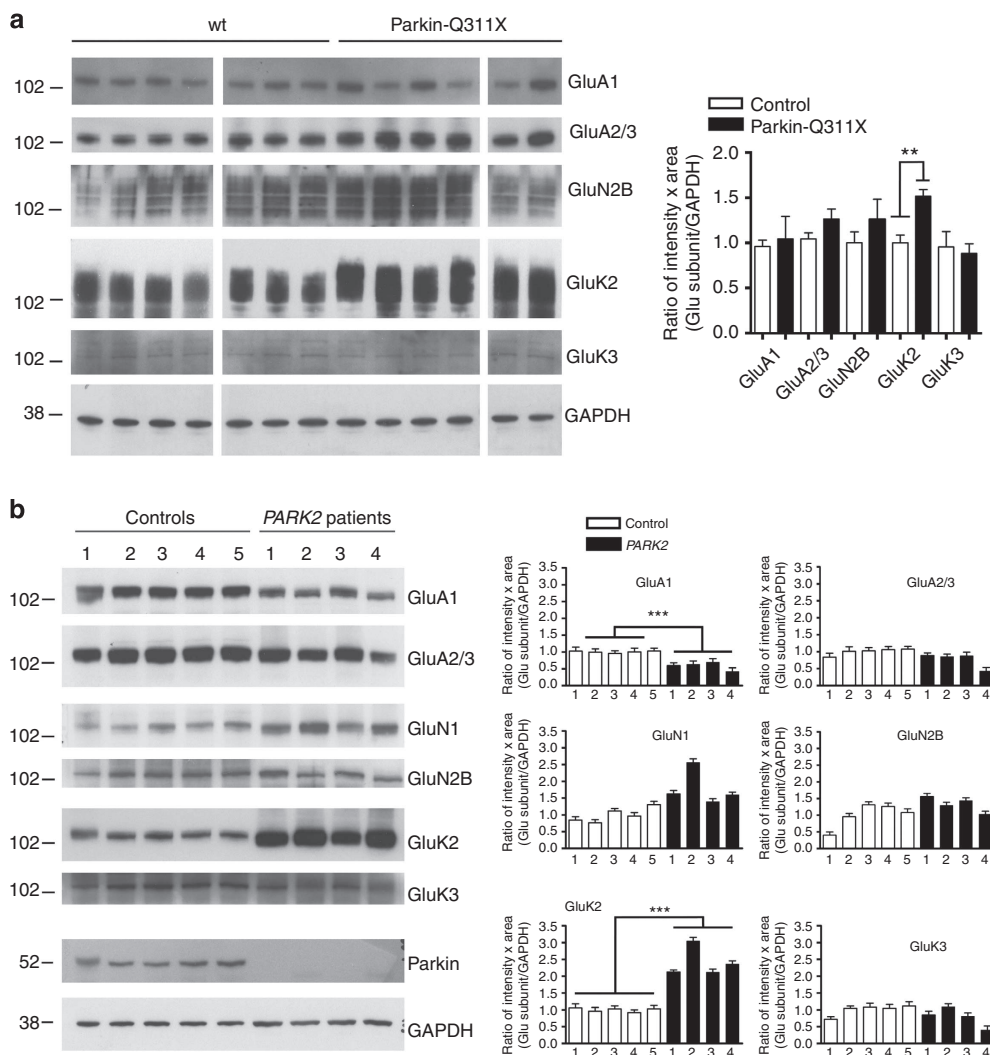


Figure 1 | Increased GluK2 levels in brain tissues from the *PARK2* mouse model parkin-Q311X and from patients with *PARK2* mutations. (a) Western blottings of glutamate receptor subunits in substantia nigra lysates from controls ($n=7$) and littermate parkin-Q311X mice ($n=6$). All mice were 3 to 4 weeks old. Samples were run in parallel gels, each gel contained wt and parkin-Q311X samples. Western blottings were blotted and developed contemporaneously. Results derive from three independent experiments. The densitometer analysis shows that GluK2 protein is significantly increased in parkin-Q311X mice as compared with littermate controls (unpaired t -test, $^{**}P=0.0010$, $t=4.424$). No statistically significant differences were found for the other AMPA, NMDA and KAR subunits analysed (unpaired t -test, $P>0.05$). No GluK1 and GluN1 expression was detectable. Error bars indicate \pm s.e.m. **(b)** Western blottings for glutamate receptor subunits in frontal cortex brain lysates from control subjects ($n=5$) and *PARK2* patients ($n=4$). No GluK1 expression was detectable. Results derive from three independent experiments. The densitometer analysis shows that GluK2 protein is significantly increased in brain tissues from patients with *PARK2* mutations (unpaired t -test; $^{***}P=0.0002$; $t=7.259$) and that GluA1 decreases in brain tissues from patients with *PARK2* mutations (unpaired t -test; $^{***}P=0.0001$; $t=7.826$). Error bars indicate \pm s.e.m.

ubiquitination, whereas transfection of the catalytically null mutant parkinC431S left GluK2a ubiquitination unchanged (controls 1.00 ± 0.12 versus wt parkin 1.79 ± 0.19 and parkinC431S 1.04 ± 0.08 , ANOVA $^{*}P=0.0219$; Fig. 3b and Supplementary Fig. 8). To investigate whether parkin can ubiquitinate endogenous GluK2, we analysed GluK2 ubiquitination in primary hippocampal neurons. We silenced endogenous parkin in primary hippocampal neurons by lentiviral infection of a GFP-shRNA-parkin construct (Supplementary Fig. 9). In these experiments, we detected a ubiquitin smear in GluK2 immunoprecipitated samples; rat parkin silencing decreased GluK2 ubiquitination, whereas co-expression of shRNA-resistant human parkin (parkin^R) increased GluK2 ubiquitination (sh-scrambled 1.00 ± 0.10 versus sh-parkin 0.51 ± 0.03 versus sh-parkin + parkin^R 0.90 ± 0.10 ; ANOVA $^{*}P=0.0169$; Fig. 3c and Supplementary Fig. 10). Hence, parkin

ubiquitinates GluK2 *in vitro*, GluK2 expressed in heterologous cell cultures and GluK2 containing KARs in cultured hippocampal neurons. Knockdown of parkin function significantly decreases endogenous GluK2 ubiquitination.

Loss of parkin increases KAR currents and excitotoxicity.

Given that KAR surface levels are regulated by GluK2 conjugation to small ubiquitin-like modifier protein-1 (ref. 15), we hypothesized that GluK2 ubiquitination by parkin could regulate KAR surface levels. We silenced endogenous parkin in primary hippocampal neurons by lentiviral infection with GFP-shRNA-parkin construct (Supplementary Fig. 9). We found that parkin silencing specifically caused accumulation of endogenous GluK2 in the plasma membrane, whereas parkin^R co-expression led to the opposite effect (sh-scrambled 1.000 ± 0.017 versus sh-parkin 2.053 ± 0.274 versus sh-parkin + parkin^R 0.991 ± 0.0572 ,

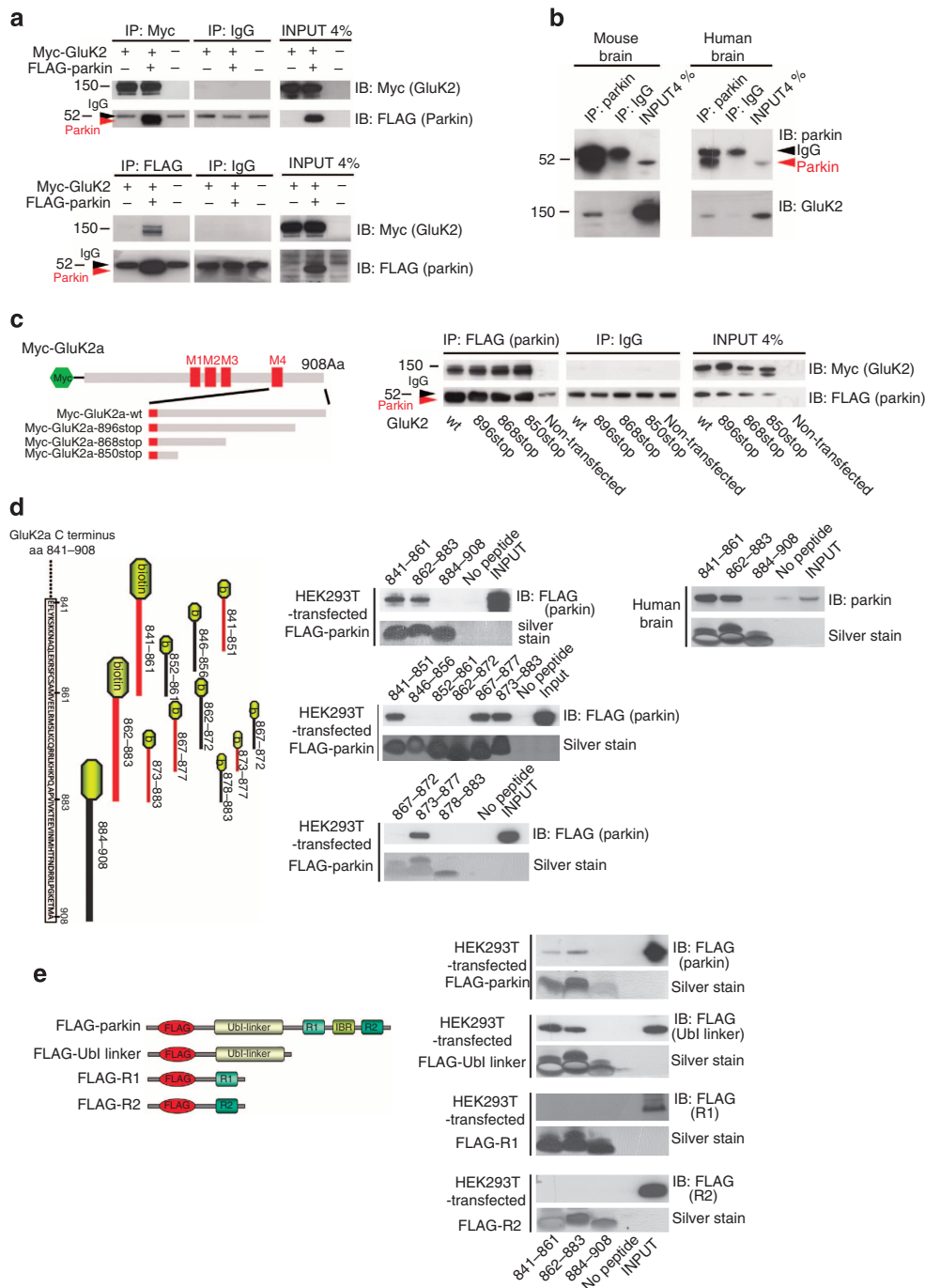


Figure 2 | Parkin interacts with GluK2. (a) Representative western blottings of co-immunoprecipitations in HEK293T cells transfected with FLAG-parkin and Myc-GluK2a. The data show that FLAG-parkin co-immunoprecipitates with Myc-GluK2a and that Myc-GluK2a co-immunoprecipitates with FLAG-parkin. The image is representative of five independent experiments. (b) Representative western blottings of co-immunoprecipitations between endogenous parkin and GluK2 in whole mouse brain lysates and whole human brain lysates. The data show that GluK2 co-immunoprecipitates with parkin. The image is representative of three independent experiments. (c) Western blottings of co-immunoprecipitation experiments from HEK293T cells transfected with FLAG-parkin and Myc-GluK2a mutants truncated at aa 896, 868 and 850. Our terminology for these truncation mutants indicates the position at which a stop codon was introduced. All the mutants were able to bind parkin. The data show that the parkin-GluK2a interaction is unaffected by the loss of the last 58 aa of the GluK2a tail. The image is representative of four independent experiments. (d) Pull-down assay using biotinylated peptides spanning the GluK2a C terminus and lysates from human brain or HEK293T cells expressing FLAG-parkin. GluK2a peptides that bind parkin are indicated in red. The image is representative of five independent experiments. (e) Pull-down assay using biotinylated GluK2a peptides and lysates from HEK293T cells expressing FLAG-parkin or amino-terminally flagged parkin domains (FLAG-Ubl-linker; FLAG-R1; FLAG-R2). GluK2a peptides pulled down FLAG-Ubl-linker of parkin. The image is representative of five independent experiments.

ANOVA $**P = 0.0053$; Fig. 4a and Supplementary Fig. 11). In addition, we co-transfected neurons with sh-parkin and Myc-GluK2a, and confirmed by immunofluorescence that parkin silencing increased surface Myc-GluK2a (sh-scrambled 1.00 ± 0.14 versus sh-parkin 1.61 ± 0.17 ; sh-parkin + parkin^R 0.93 ± 0.14 ; ANOVA $**P = 0.0066$; Fig. 4b).

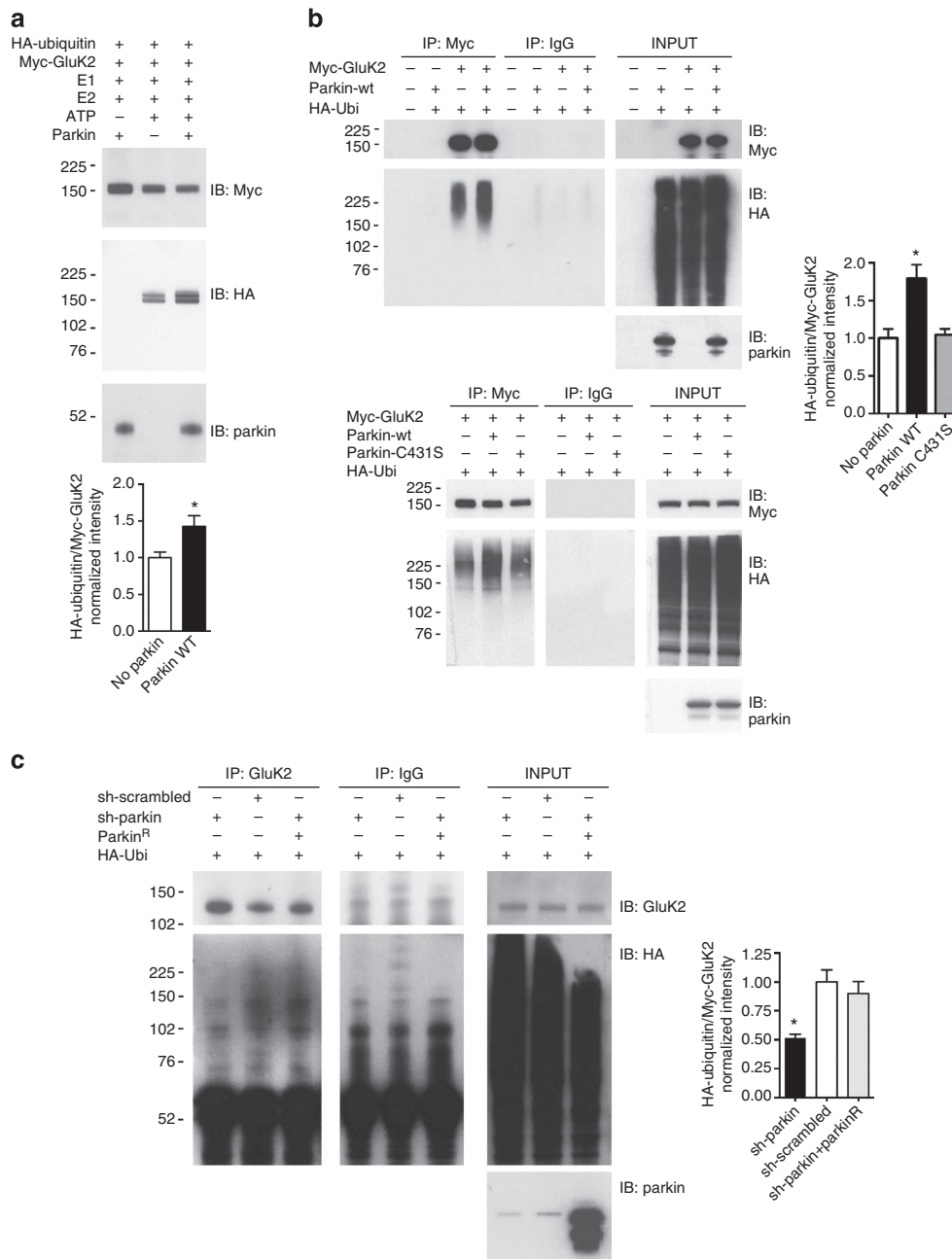


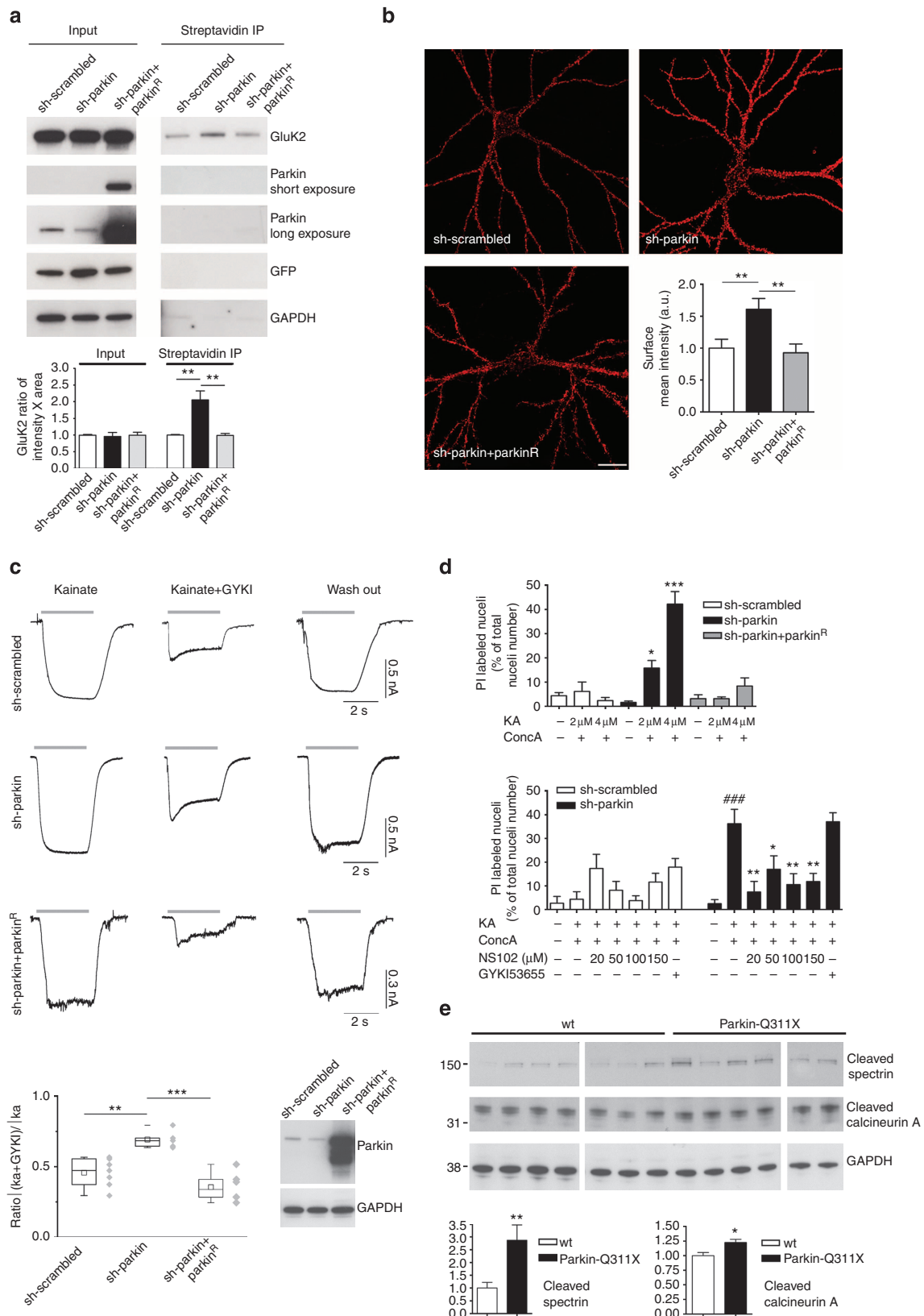
Figure 3 | Parkin ubiquitinates GluK2. (a) *In vitro* ubiquitination assay of Myc-GluK2a using recombinant E1 (human ubiquitin-activating enzyme E1), recombinant E2 (UbcH7), HA-ubiquitin and parkin. Myc-GluK2a was slightly ubiquitinated in the presence of E1 and E2 alone but recombinant parkin significantly increased GluK2a ubiquitination. Results are representative of nine independent experiments (two-tailed unpaired *t*-test, **P* = 0.0201, *t* = 2.580, *df* = 16). Error bars indicate ± s.e.m. (b) Western blotting of co-immunoprecipitation using HEK293T cells transfected with Myc-GluK2a, HA-ubiquitin, wt parkin or parkin C431S. GluK2a was ubiquitinated in HEK293T cells and parkin transfection significantly increased GluK2a ubiquitination. Parkin C431S transfection did not increase GluK2a ubiquitination. Results are representative of three independent experiments (one-way analysis of variance (ANOVA) and Tukey test, **P* = 0.0219, *F* = 9.029). Error bars indicate ± s.e.m. (c) Western blotting of co-immunoprecipitation using primary hippocampal neurons transfected with HA-ubiquitin and infected with lentiviral particle encoding sh-parkin or sh-scrambled, or sh-parkin + parkin^R. Endogenous parkin silencing significantly decreased endogenous GluK2 ubiquitination. Parkin^R overexpression rescued endogenous GluK2 ubiquitination. The image is representative of three independent experiments that gave identical results (one-way ANOVA and Tukey test, **P* = 0.0169, *F* = 8.689). Error bars indicate ± s.e.m.

Loss of parkin function was reported to enhance glutamatergic synapse efficacy⁶. Here we tested a specific regulation of KAR function by parkin. We recorded currents evoked by kainate application in cultured hippocampal neurons. To isolate KAR-mediated currents evoked by kainate, we used GYKI 53655 (10 μM), a non-competitive AMPAR antagonist that does not

affect KARs¹⁶. KAR-mediated currents evoked in hippocampal neurons expressing sh-parkin had higher amplitude than those evoked in neurons expressing sh-scrambled. Co-transfection with parkin^R decreased KAR-mediated currents (ratio between current intensity on kainate + GYKI 53655/kainate alone: sh-scrambled 0.4579 ± 0.03769; sh-parkin 0.6790 ± 0.03642;

sh-parkin + parkin^R 0.3555 ± 0.04194; ANOVA ***P* < 0.01 sh-scrambled versus sh-parkin; ANOVA ****P* < 0.001 sh-parkin versus sh-parkin + parkin^R, Fig. 4c). These data show that loss of parkin function increases the level of endogenous KARs, thus resulting in increased KAR currents evoked by kainate.

We next tested whether the KAR currents increase resulting from the loss of endogenous parkin increased neuron vulnerability to excitotoxicity. We measured cell death rates in primary hippocampal neurons treated with moderate kainate concentrations (2–4 μM) plus concanavalin A (200 μg ml⁻¹), a lectin that



specifically blocks KAR desensitization. Kainate plus concanavalin A induced dose-dependent cell death selectively in sh-parkin neurons (kainate $2\ \mu\text{M}$ + ConCA $200\ \mu\text{g ml}^{-1}$: sh-scrambled 6.15 ± 3.90 versus sh-parkin 15.80 ± 3.12 , ANOVA $*P < 0.05$; kainate $4\ \mu\text{M}$: sh-scrambled 2.40 ± 1.29 versus sh-parkin 42.21 ± 5.20 , ANOVA $***P < 0.001$). Co-transfection with parkin^R rescued neuronal cell death (kainate $2\ \mu\text{M}$ + ConCA $200\ \mu\text{g ml}^{-1}$: sh-parkin + parkin^R 3.20 ± 1.56 ; kainate $4\ \mu\text{M}$ + ConCA $200\ \mu\text{g ml}^{-1}$: sh-parkin + parkin^R 8.39 ± 3.38). Co-treatment with KAR antagonist NS102 (ref. 17) (20 – $150\ \mu\text{M}$) rescued cell death (value for sh-parkin: kainate $4\ \mu\text{M}$ + ConCA $200\ \mu\text{g ml}^{-1}$, 36.20 ± 6.07 versus untreated 2.56 ± 1.73 , ANOVA $###P < 0.001$; kainate $4\ \mu\text{M}$ + ConCA $200\ \mu\text{g ml}^{-1}$ + NS102 $20\ \mu\text{M}$ 7.46 ± 4.44 , ANOVA $**P < 0.01$ versus kainate $4\ \mu\text{M}$ + ConCA $200\ \mu\text{g ml}^{-1}$; kainate $4\ \mu\text{M}$ + ConCA $200\ \mu\text{g ml}^{-1}$ + NS102 $50\ \mu\text{M}$ 17.01 ± 5.72 , ANOVA $*P < 0.05$ versus kainate $4\ \mu\text{M}$ + ConCA $200\ \mu\text{g ml}^{-1}$; kainate $4\ \mu\text{M}$ + ConCA $200\ \mu\text{g ml}^{-1}$ + NS102 $100\ \mu\text{M}$ 10.58 ± 4.57 , ANOVA $**P < 0.01$ versus kainate $4\ \mu\text{M}$ + ConCA $200\ \mu\text{g ml}^{-1}$; kainate $4\ \mu\text{M}$ + ConCA $200\ \mu\text{g ml}^{-1}$ + NS102 $150\ \mu\text{M}$ 11.84 ± 3.41 ANOVA $**P < 0.01$ versus kainate $4\ \mu\text{M}$ + ConCA $200\ \mu\text{g ml}^{-1}$). Co-treatment with the AMPAR antagonist GYKI53655 did not rescue cell death (value for sh-parkin: kainate $4\ \mu\text{M}$ + ConCA $200\ \mu\text{g ml}^{-1}$ + GYKI53655 $10\ \mu\text{M}$ 37.05 ± 3.80 , ANOVA $P > 0.05$ versus kainate $4\ \mu\text{M}$ + ConCA $200\ \mu\text{g ml}^{-1}$; Fig. 4d). Hence, these data show that loss of parkin function increases the vulnerability of hippocampal neurons to KAR-dependent excitotoxicity.

To test whether the increased GluK2 levels were associated with increased vulnerability to excitotoxicity *in vivo*, we analysed neuronal levels of cleaved spectrin (non-erythroid alpha II-spectrin) and cleaved calcineurin A, both well-recognized markers for excitotoxic damage^{18–20}. Cleaved spectrin and cleaved calcineurin A were significantly higher in substantia nigra of parkin-Q311X mice than in littermate controls (cleaved spectrin: wt 1.00 ± 0.22 versus parkin-Q311X 2.87 ± 0.60 , unpaired *t*-test $**P = 0.0096$; cleaved calcineurin A: wt 1.00 ± 0.05 versus parkin-Q311X 1.23 ± 0.05 , unpaired *t*-test $*P = 0.0124$; Fig. 4e and Supplementary Fig. 12). Hence, the increased GluK2 levels and excitotoxicity markers in our experiments disclosed in substantia nigra of parkin-Q311X mice suggest that KAR upregulation induces excitotoxicity *in vivo*.

Discussion

In this study, we describe major new findings that extend our current knowledge about the molecular mechanism through which parkin regulates glutamatergic synapses⁶. Parkin interacts with and ubiquitinates the GluK2 KAR subunit and regulates GluK2 levels and KAR currents. A loss of parkin function increases KAR-dependent excitotoxicity *in vitro* and mutant parkin expression correlates with GluK2 accumulation and excitotoxicity features *in vivo*. Besides showing that parkin regulates KAR currents, we specify that it does so by binding to the GluK2 C-terminal cytoplasmic tail. Parkin-GluK2 binding appears as a transient effect dependent on KAR activation by agonists. As parkin affects somatodendritic KAR currents, the parkin-GluK2 interaction probably takes place at post-synaptic sites. Given that parkin is also localized in axons²¹, we cannot exclude the possibility that parkin regulates pre-synaptic GluK2-containing KARs, which are involved in the facilitation of synaptic transmission²². GluK2a interacts with Ubl-linker domain of parkin, similar to other parkin substrates²³. The accumulation of GluK2 we found in brains from patients with *PARK2* mutations and in the *PARK2* mouse model parkin-Q311X further indicates that GluK2 is a ‘genuine’ parkin substrate. By identifying GluK2 as a parkin substrate, our results add to the evidence that parkin can ubiquitinate synaptic proteins^{8,24,25}. As parkin activation is a multistep process involving relocalization and release of ubiquitination activity, which are probably regulated through phosphorylation or cysteine modification, or ligand binding to the Ubl domain^{26,27}, we can speculate that GluK2 binding to Ubl domain may induce parkin activation.

The loss of parkin function increases surface and total GluK2 levels, and consistently increases KAR currents. These data agree with previous findings demonstrating that a loss of endogenous parkin increases excitatory synaptic transmission⁶. By identifying KAR as a direct target of parkin, our results provide a step ahead towards understanding the mechanism through which parkin modulates synaptic functions.

Our molecular findings also provide new insights into the mechanisms responsible for neurodegeneration in patients with ARJP. Similar to sporadic Parkinson’s disease, ARJP typically causes massive dopaminergic neuronal depletion in the substantia nigra pars compacta (SNc)²⁸, a brain region receiving glutamatergic inputs from cortex, pedunculo-pontine nuclei²⁹, superior colliculus³⁰, thalamus³¹ and subthalamic nucleus (STN).

Figure 4 | Loss of parkin function increases surface GluK2 levels, KAR currents and causes excitotoxicity. (a) Surface biotinylation assay in hippocampal neurons infected with lentivirus encoding sh-scrambled or sh-parkin, or sh-parkin + parkin^R. Endogenous parkin silencing increased surface GluK2 levels; co-infection with lentivirus encoding parkin^R rescued GluK2 surface levels (one-way analysis of variance (ANOVA)–Dunnett’s multiple comparison test, $***P = 0.0053$, $F = 14.25$). (b) Surface Myc labelling in hippocampal neurons co-transfected with sh-parkin + Myc-GluK2a or sh-scrambled + Myc-GluK2a, or sh-parkin + parkin^R + Myc-GluK2a (one-way ANOVA–Bonferroni test, $**P = 0.0066$, $F = 6.082$, 29 degrees of freedom; ten neurons analysed/each condition). Scale bar, $20\ \mu\text{m}$. (c) KAR current analysis in hippocampal neurons infected with lentivirus encoding GFP bicistronic sh-scrambled or sh-parkin, or sh-parkin + parkin^R. Whole-cell responses were induced by rapid application of $100\ \mu\text{M}$ kainate. To isolate KAR currents from those resulting from AMPAR opening, we added $10\ \mu\text{M}$ GYKI 53655 ($\text{IC}_{50} = 0.9 \pm 0.08\ \mu\text{M}$)¹⁶. Responses are shown before application (left panel), during the concomitant application of GYKI53655 (central panel) and after GYKI53655 washout (right panel). Western blotting shows parkin expression in the three experimental conditions. The chart plot shows the ratio between current stimulated by kainate + GYKI53655 and the current triggered by 3 s application of kainate alone (one-way ANOVA and Tukey test, $**P < 0.01$; $***P < 0.001$; $F = 15.87$). Error bars indicate 25th and 75th percentiles. (d) Primary hippocampal neurons were infected with lentivirus encoding GFP bicistronic sh-scrambled or sh-parkin, or sh-parkin + parkin^R. Data represent the percentage of infected cells (green fluorescent cells) labelled by propidium iodide (PI). Kainate 2 – $4\ \mu\text{M}$ or concanavalin A $200\ \mu\text{g ml}^{-1}$ alone did not induce cell death. Kainate 2 – $4\ \mu\text{M}$ + concanavalin A $200\ \mu\text{g ml}^{-1}$ caused excitotoxicity in parkin-silenced cells. Co-infection with lentivirus encoding parkin^R rescued cell death (one-way ANOVA–Tukey test, $*P < 0.05$ versus sh-scrambled $2\ \mu\text{M}$ kainate; $***P < 0.001$ versus sh-scrambled $4\ \mu\text{M}$ kainate; $F = 20.02$). NS102 20 – $150\ \mu\text{M}$ blocked excitotoxicity in parkin-silenced neurons (one-way ANOVA–Dunnett’s multiple comparison test, $*P < 0.05$, $**P < 0.01$, versus kainate treated; $###P < 0.001$ versus untreated, $F = 7.268$). GYKI53655 ($10\ \mu\text{M}$) did not rescue cell death. (e) Western blottings for cleaved spectrin and cleaved calcineurin A in substantia nigra lysates from 3-week-old controls ($n = 7$) and littermate parkin-Q311X mice ($n = 6$). Results derive from three independent experiments (unpaired *t*-test, $**P = 0.0096$, $t = 3.128$ for cleaved spectrin; $*P = 0.0124$, $t = 2.941$ for cleaved calcineurin A). All error bars in Fig. 4 histograms indicate \pm s.e.m.

These brain anatomical connections make the SNc neurons highly vulnerable to glutamate and suggested the longstanding hypothesis that SNc neuron depletion in Parkinson's disease may stem from excitotoxicity^{32,33}. SNc neurons abundantly express KAR subunits³⁴. Although KAR function in the SNc remains elusive, our findings, showing that a loss of parkin function increases KAR function, support the excitotoxicity hypothesis in parkin-related ARJP. Current knowledge shows that in parkinsonian patients' brain, the STN displays irregular burst firing deriving from dopamine deficiency³², resulting in high release of glutamate in the SNc, thereby causing excitotoxic damage^{33,35}. In this context, a parkin loss of function may cause primary excitotoxic damage that would transiently precede the excitotoxic damage, depending on the overactivity in the STN glutamatergic neurons.

Hence, our results, suggesting that parkin modulates excitatory currents by binding to and promoting GluK2 ubiquitination, support the hypothesis that a loss of neuronal parkin increases vulnerability to excitotoxicity⁶ and suggest that patients with the *PARK2* mutation might benefit from neuroprotective therapy targeting KAR.

Methods

Glutamate receptor subunit analysis in mouse brain tissues. Parkin-Q311X (A) mice and littermate controls (all mice were female FVB/N strain) were purchased from Charles River (Calco, Italy). Mice were kept under environmentally controlled conditions on a 12-h light/dark cycle with food and water *ad libitum*. Three- to four-week-old mice were killed and the substantia nigra were immediately dissected out on ice. Tissues were homogenized with lysis buffer (20 mM Tris, pH 7.5, 150 mM NaCl, 1 mM EDTA, 1 mM EGTA, 1% Triton X-100, protease inhibitors (Roche), 50 μ M MG132 and 10 mM N-ethylmaleimide (Sigma)). Western blottings were performed with Novex NuPAGE SDS-PAGE gels (Invitrogen). The following antibodies were used: GluA1 (13185, Cell Signaling, 1:500), GluA2/3 (AB1506, Millipore, 1:1,000), GluN2B (PA5-18536, Thermo Scientific, 1:300), GluK2 (TA310550, Origene, 1:1,000) and GluK3 (H0002899, Abnova, 1:2,000), GAPDH (sc-25778, Santa Cruz, 1:1,000), Calcineurin A (ADI-SPA-610, Enzo Life Sciences 1:1,000) and Spectrin (2122, Cell Signaling, 1:1,000). The study was approved by The Ethics Committees of IRCCS Istituto Auxologico Italiano "Comitato Etico dell'IRCCS Istituto Auxologico Italiano di Milano". Experimental procedures took place in accordance with the European Communities Council Directive (86/809/EEC).

Glutamate receptor subunit analysis in human brain tissues. Control and *PARK2* post-mortem brain tissues were from the Department of Neurology, Juntendo University School of Medicine. The study protocol was approved by the Human Ethics Review Committee at Juntendo University School of Medicine. Informed consent to use human tissues were obtained from patients or close family members. Patients' data are reported in Supplementary Table 1. Control brain tissues were autopsied brain tissue from age-matched controls who had undergone neuropathological examination to exclude neurodegenerative disorders. Tissues were homogenized with lysis buffer (20 mM Tris, pH 7.5, 150 mM NaCl, 1 mM EDTA, 1 mM EGTA, 1% Triton X-100, protease inhibitors (Roche), 50 μ M MG132 and 10 mM N-ethylmaleimide (Sigma)). Western blottings were performed with Novex NuPAGE SDS-PAGE gels (Invitrogen). The following antibodies were used: GluA1 ((13185, Cell Signaling, 1:500), GluA2/3 (AB1506, Millipore, 1:1,000), GluN1 (clone N308/48, NeuroMab, 1:300), GluN2B (PA5-18536, Thermo Scientific, 1:300), GluK1 and GluK3 (H0002897 and H0002899, respectively, Abnova, 1:2,000), GluK2 (TA310550, Origene, 1:1,000), parkin (P6248, Sigma, 1:6,000), GAPDH (sc-25778, Santa Cruz, 1:1,000).

Analysis of GluK2-parkin interaction. Plasmids encoding complementary DNA for human parkin and parkin domains (Ubl-linker, aa 1–237; RING1, aa 217–310; RING2, aa 395–465) were described previously³⁶. Plasmids encoding truncated GluK2 mutants were created by mutagenizing the Myc-GluK2a(R) plasmid³⁷ using the QuikChange mutagenesis kit (Stratagene). Samples were immunoprecipitated as described³⁸ according to the following protocol: 500 μ g of sample were pre-cleared by adding 50 μ l of washed Protein A or G agarose bead slurry (catalogue number 17-5138-01 and 17-0618-01, GE Healthcare). The agarose beads were collected by pulsing 5 s in the microcentrifuge at 14,000 g and discarded. Sample supernatants were incubated with Myc antibody (R950, Invitrogen, 1:500) or parkin antibody (P6248, Sigma, 1:1,000), or FLAG antibody (M2, Sigma, 1:500) at 4 °C overnight. Fifty microlitres of washed Protein A or G agarose bead slurry were added to the reaction mixture and gently rocked at 4 °C for additional 2 h. The agarose beads were then collected by pulsing 5 s in the microcentrifuge at 14,000 g

and washed three times with ice-cold washing buffer (20 mM Tris, pH 7.5, 500 mM NaCl, 1 mM EDTA, 1 mM EGTA, 1% Triton X-100, protease inhibitors (Roche), 50 μ M MG132). The beads were resuspended in 40 μ l of 2 \times Laemmli sample buffer, boiled, analysed by SDS-PAGE with Novex NuPAGE SDS-PAGE gels (Invitrogen).

For pull-down experiments, lysates (150 μ g) were incubated overnight at 4 °C with 15 μ g of biotinylated peptide (Primm srl) previously conjugated to streptavidin-conjugated magnetic beads (Invitrogen), washed in lysis buffer, resuspended in SDS sample buffer and boiled. Gels were silver-stained with the SilverQuest Silver Staining Kit (Invitrogen). Parkin was labelled by parkin antibody (P6248, Sigma) or FLAG antibody (M2, Sigma).

FRET analysis. Parkin cDNA was subcloned into a pECFP-C1 vector (Clontech). The plasmid encoding GluK2a C-terminally conjugated to enhanced yellow fluorescence protein (YFP) has been previously described³⁹. FRET videos were acquired with an AF6000 microscope (Leica) equipped with a FRET excitation and emission fast filter wheel and a \times 100 oil objective at a rate of one frame per minute. Each frame was acquired on three channels: CFP excitation and CFP emission (CFP), CFP excitation and YFP emission (FRET), and YFP excitation and YFP emission (YFP). FRET efficiency was calculated pixel-by-pixel according to the following formula (1):

$$E_A(i) = \frac{B - A \times \beta - C \times \gamma}{C}$$

where *A*, is the fluorescence intensity measured in the CFP channel, and *B* and *C* are the fluorescence intensities measured in the FRET and YFP channels, whereas β and γ are correction factors for the spectral bleed throughout our constructs (Leica LAS AF software method 1). FRET efficiency increase was calculated by comparing the FRET efficiency distribution for three frames before and after treating for 10 min with 10 mM glutamate.

Ubiquitination assays. For *in vitro* ubiquitination assay, purified Myc-tagged GluK2 (1 μ M, Origene) was incubated in ubiquitination assay buffer (10 \times buffer, 5 mM Mg-ATP, 1 mM dithiothreitol and 20 U ml⁻¹ pyrophosphatase; Biomol) together with 100 nM recombinant human ubiquitin-activating enzyme E1 (Biomol), 2.5 μ M recombinant E2 UbcH7 (Biomol), 2.5 μ M haemagglutinin (HA)-tagged ubiquitin and 100 nM recombinant His-tagged parkin (Boston Biochem) for 2 h at 37 °C. The samples were immunoprecipitated with Myc antibody (R950, Invitrogen) and analysed by western blotting.

For ubiquitination assay in HEK293T, cells were transfected with plasmid encoding human parkin wt, parkin C431S, MycGluK2a plasmid and HA-ubiquitin. Cells lysates were immunoprecipitated with Myc antibody (R950, Invitrogen). Immunoprecipitated samples were analysed by western blotting with horseradish peroxidase-conjugated antibody against Myc (R951-25, Invitrogen) and HA (130-091-972, Miltenyi Biotec).

For analysis of endogenous GluK2 ubiquitination in primary neurons, lysates were immunoprecipitated with anti GluK2/3 antibody (clone NL9 Millipore) according to the manufacturer's protocol. Five hundred micrograms of sample were pre-cleared by adding 50 μ l of washed Protein A agarose bead slurry (catalogue number 17-5138-01, GE Healthcare). The agarose beads were collected by pulsing 5 s in the microcentrifuge at 14,000 g and discarded. Sample supernatants were incubated with 7.5 μ l of anti-GluK2/3 at 4 °C overnight. Fifty microlitres of washed Protein A agarose bead slurry were added to the reaction mixture and gently rocked at 4 °C for additional 2 h. The agarose beads were then collected by pulsing 5 s in the microcentrifuge at 14,000 g and washed three times with ice-cold washing buffer (20 mM Tris, pH 7.5, 500 mM NaCl, 1 mM EDTA, 1 mM EGTA, 1% Triton X-100, protease inhibitors (Roche), 50 μ M MG132). The beads were resuspended in 40 μ l of 2 \times Laemmli sample buffer, boiled, analysed by SDS-PAGE with Novex NuPAGE SDS-PAGE gels (Invitrogen) and developed with an antibody against HA (H6908, Sigma, 1:1,000).

Lentiviral infections in neurons. Primary rat hippocampal neurons were prepared from embryonic day 18–19 rat brains³⁸ and plated on poly-D-lysine (30 μ g ml⁻¹)-coated coverslips at densities of 75,000 cells per well for immunocytochemistry, 300,000 cells per well for biochemistry experiments and 150,000 cells per well for electrophysiological experiments. Neurons were infected with lentivirus at Days in Vitro (DIV) 8 (ref. 40). The pRNAT plasmid encoding short hairpin RNA (shRNA) specific against rat parkin and scrambled have been previously described⁶: parkin shRNA sequence was 5'-CCAAACCGGATGAGTGGAGAGT GCCAATC-3'. The same shRNA sequences were subcloned into the pLVTHM plasmid and used to prepare lentiviral particles. Rescue experiments were performed by expression of human parkin cDNA.

Biotinylation assay and immunofluorescence in neurons. Plasma membrane proteins were biotinylated using membrane-impermeant sulfo-NHS-SS-biotin (0.3 mg ml⁻¹, Pierce) for 5 min at 37 °C. Labelled neurons were washed with TBS supplemented with 0.1 mM CaCl₂, 1.0 mM MgCl₂ and 50 mM glycine. After further washes with TBS supplemented with 0.1 mM CaCl₂ and 1.0 mM MgCl₂ on ice, the cells were lysed in extraction buffer (50 mM Tris-HCl, pH 7.4, 1 mM EDTA,

150 mM NaCl, 1% SDS and protease inhibitor mixture). Lysates were boiled for 5 min and immunoprecipitated with streptavidin-conjugated magnetic beads (Dynabeads, Invitrogen).

For immunofluorescence, neurons were transfected at DIV 13–14 with the Myc-GluK2a(R) plasmid using the calcium phosphate method⁴⁰. For surface staining, live DIV 18 hippocampal neurons were incubated for 10 min at 37 °C with Myc antibody. After washing (PBS supplemented with 1 mM MgCl₂ and 0.1 mM CaCl₂), neurons were fixed for 7 min at room temperature in 4% paraformaldehyde/4% sucrose without permeabilization and stained with a Cy3-conjugated secondary antibody (Invitrogen) applied in gelatin detergent buffer (30 mM phosphate buffer at pH 7.4 containing 0.2% gelatin, 0.5% Triton X-100 and 0.8 M NaCl). Fluorescent images were acquired and quantified⁴⁰: labelled transfected neurons were chosen randomly for quantification from four coverslips from five independent experiments for each construct. Fluorescence images were acquired with a Biorad MRC1024 confocal microscope, using a Nikon ×60 objective with sequential acquisition setting at 1,280 × 1,024 pixel resolution. All morphometric measurements were made with Metamorph image analysis software (Universal Imaging Corporation). Both image acquisition and morphometric quantification were performed by investigators who were 'blind' to the experimental condition.

KAR current recording in *in vitro* neurons. Whole-cell patch-clamp data were recorded from DIV 19–21 primary hippocampal neurons (clamped at –70 mV). The coverslips were perfused with the following extracellular solution (mM): 140 NaCl, 3 KCl, 2 CaCl₂, 1.2 MgCl₂, 10 glucose and 10 HEPES (pH 7.4). Borosilicate glass pipettes (5–8 MΩ resistance) were filled with the following solution (mM): 126 K-gluconate, 4 NaCl, 10 HEPES, 10 glucose, 1 MgSO₄, 0.5 CaCl₂, 1 EGTA, 3 ATP-Mg and 0.1 GTP-Na (pH 7.2). Recordings were accepted for analysis when membrane resistance (R_m) was >150 MΩ, series resistance (R_s) was <15 MΩ and, together with membrane capacitance (C_m), they changed by no more than 10% from the original value during the recording. Holding currents were lower than –100 pA and remained significantly unchanged throughout the experiments (R_m = 268 ± 31 MΩ, R_s = 9.1 ± 0.6 MΩ, C_m = 42.2 ± 2.3 pF and holding current –39.0 ± 5.2 pA). Signals were derived using a Multiclamp 700B amplifier (Axon Instruments), digitized through a Digidata 1440A interface (Axon Instruments) and acquired for online visualization and offline analysis using pClamp10 Software (Axon Instruments). Data were recorded at 28–30 °C using a TC-324B temperature control (Warner Instruments).

Excitotoxicity assay. Neurons were infected at DIV 8 with green fluorescent protein (GFP) sh-scrambled or sh-parkin or sh-parkin + parkin^R. One week after infection, neurons were treated as indicated in Fig. 4d. Eight hours after the treatment, neurons were washed in standard neurobasal medium and then incubated with 1 μg ml⁻¹ of propidium iodide for 10 min. Coverslips were PBS washed, fixed with 4% paraformaldehyde for 10 min and mounted with ProLong mounting DAPI (4',6-diamidino-2-phenylindole) (Invitrogen, P36931). Images were acquired at confocal microscopy (Nikon Eclipse C1) and neurons were counted in ten fields from each coverslip. The percentage of dead neurons was calculated as the ratio between red-labelled neurons (propidium iodide) and green fluorescent cells (GFP infected). Approximately 800 to 1,300 neurons were scored for each condition. Experiments were repeated three times each on three separate cultures.

Statistical analysis. Statistical analyses were performed using GraphPad Prism4 software. Data were subjected to normality test (Kolmogorov-Smirnov test). Student's *t*-test was used to compare two groups and one-way analysis of variance followed by appropriate *post-hoc* tests was used to compare multiple groups. Data are presented as mean ± s.e.m.

References

- Kitada, T. *et al.* Mutations in the parkin gene cause autosomal recessive juvenile parkinsonism. *Nature* **392**, 605–608 (1998).
- Tan, E. K. & Skipper, L. M. Pathogenic mutations in Parkinson disease. *Hum. Mutat.* **28**, 641–653 (2007).
- Shimura, H. *et al.* Familial Parkinson disease gene product, parkin, is a ubiquitin-protein ligase. *Nat. Genet.* **25**, 302–305 (2000).
- Vives-Bauza, C. & Przedborski, S. Mitophagy: the latest problem for Parkinson's disease. *Trends Mol. Med.* **17**, 158–165 (2011).
- Youle, R. J. & Narendra, D. P. Mechanisms of mitophagy. *Nat. Rev. Mol. Cell Biol.* **12**, 9–14 (2011).
- Helton, T. D., Otsuka, T., Lee, M. C., Mu, Y. & Ehlers, M. D. Pruning and loss of excitatory synapses by the parkin ubiquitin ligase. *Proc. Natl Acad. Sci. USA* **105**, 19492–19497 (2008).
- Fallon, L. *et al.* Parkin and CASK/LIN-2 associate via a PDZ-mediated interaction and are co-localized in lipid rafts and postsynaptic densities in brain. *J. Biol. Chem.* **277**, 486–491 (2002).
- Joch, M. *et al.* Parkin-mediated monoubiquitination of the PDZ protein PICK1 regulates the activity of acid-sensing ion channels. *Mol. Biol. Cell* **18**, 3105–3118 (2007).
- Trempe, J. F. *et al.* SH3 domains from a subset of BAR proteins define a Ubl-binding domain and implicate parkin in synaptic ubiquitination. *Mol. Cell* **36**, 1034–1047 (2009).
- Staropoli, J. F. *et al.* Parkin is a component of an SCF-like ubiquitin ligase complex and protects postmitotic neurons from kainate excitotoxicity. *Neuron* **37**, 735–749 (2003).
- Hattori, N. *et al.* Molecular genetic analysis of a novel Parkin gene in Japanese families with autosomal recessive juvenile parkinsonism: evidence for variable homozygous deletions in the Parkin gene in affected individuals. *Ann. Neurol.* **44**, 935–941 (1998).
- Lu, X. H. *et al.* Bacterial artificial chromosome transgenic mice expressing a truncated mutant parkin exhibit age-dependent hypokinetic motor deficits, dopaminergic neuron degeneration, and accumulation of protease K-resistant alpha-synuclein. *J. Neurosci.* **29**, 1962–1976 (2009).
- Coussen, F. & Mülle, C. Kainate receptor-interacting proteins and membrane trafficking. *Biochem. Soc. Trans.* **34**, 927–930 (2006).
- Shimura, H. *et al.* Ubiquitination of a new form of alpha-synuclein by parkin from human brain: implications for Parkinson's disease. *Science* **293**, 263–269 (2001).
- Martin, S., Nishimune, A., Mellor, J. R. & Henley, J. M. SUMOylation regulates kainate-receptor-mediated synaptic transmission. *Nature* **447**, 321–325 (2007).
- Paternain, A. V., Morales, M. & Lerma, J. Selective antagonism of AMPA receptors unmasks kainate receptor-mediated responses in hippocampal neurons. *Neuron* **14**, 185–189 (1995).
- Verdoorn, T. A., Johansen, T. H., Drejer, J. & Nielsen, E. O. Selective block of recombinant glur6 receptors by NS-102, a novel non-NMDA receptor antagonist. *Eur. J. Pharmacol.* **269**, 43–49 (1994).
- Harris, A. S. & Morrow, J. S. Proteolytic processing of human brain alpha spectrin (fodrin): identification of a hypersensitive site. *J. Neurosci.* **8**, 2640–2651 (1988).
- Staszewski, R. D. & Yamamoto, B. K. Methamphetamine-induced spectrin proteolysis in the rat striatum. *J. Neurochem.* **96**, 1267–1276 (2006).
- Wu, H. Y. *et al.* Critical role of calpain-mediated cleavage of calcineurin in excitotoxic neurodegeneration. *J. Biol. Chem.* **279**, 4929–4940 (2004).
- Wang, X. *et al.* PINK1 and parkin target miro for phosphorylation and degradation to arrest mitochondrial motility. *Cell* **147**, 893–906 (2011).
- Contractor, A., Mülle, C. & Swanson, G. T. Kainate receptors coming of age: milestones of two decades of research. *Trends Neurosci.* **34**, 154–163 (2011).
- Spratt, D. E., Walden, H. & Shaw, G. S. RBR E3 ubiquitin ligases: new structures, new insights, new questions. *Biochem. J.* **458**, 421–437 (2014).
- Zhang, Y. *et al.* Parkin functions as an E2-dependent ubiquitin-protein ligase and promotes the degradation of the synaptic vesicle-associated protein, CDCrel-1. *Proc. Natl Acad. Sci. USA* **97**, 13354–13359 (2000).
- Choi, P. *et al.* SEPT5_v2 is a parkin-binding protein. *Brain Res. Mol. Brain Res.* **117**, 179–189 (2003).
- Trempe, J. F. *et al.* Structure of parkin reveals mechanisms for ubiquitin ligase activation. *Science* **340**, 1451–1455 (2013).
- Wauer, T. & Komander, D. Structure of the human Parkin ligase domain in an autoinhibited state. *EMBO J.* **32**, 2099–2112 (2013).
- Dawson, T. M. Unraveling the role of defective genes in Parkinson's disease. *Parkinsonism Relat. Disord.* **13**, S248–S249 (2007).
- Lavoie, B. & Parent, A. Pedunculopontine nucleus in the squirrel monkey: cholinergic and glutamatergic projections to the substantia nigra. *J. Comp. Neurol.* **344**, 232–241 (1994).
- Comoli, E. *et al.* A direct projection from superior colliculus to substantia nigra for detecting salient visual events. *Nat. Neurosci.* **6**, 974–980 (2003).
- Sadikot, A. F., Parent, A., Smith, Y. & Bolam, J. P. Efferent connections of the centromedian and parafascicular thalamic nuclei in the squirrel monkey: a light and electron microscopic study of the thalamostriatal projection in relation to striatal heterogeneity. *J. Comp. Neurol.* **320**, 228–242 (1992).
- Lozano, A. M., Dostrovsky, J., Chen, R. & Ashby, P. Deep brain stimulation for Parkinson's disease: disrupting the disruption. *Lancet Neurol.* **1**, 225–231 (2002).
- Olanow, C. W. & Tatton, W. G. Etiology and pathogenesis of Parkinson's disease. *Annu. Rev. Neurosci.* **22**, 123–144 (1999).
- Bischoff, S., Barhanin, J., Bettler, B., Mülle, C. & Heinemann, S. Spatial distribution of kainate receptor subunit mRNA in the mouse basal ganglia and ventral mesencephalon. *J. Comp. Neurol.* **379**, 541–562 (1997).
- Rodriguez, M. C., Obeso, J. A. & Olanow, C. W. Subthalamic nucleus-mediated excitotoxicity in Parkinson's disease: a target for neuroprotection. *Ann. Neurol.* **44**, S175–S188 (1998).
- Yang, F. *et al.* Parkin stabilizes microtubules through strong binding mediated by three independent domains. *J. Biol. Chem.* **280**, 17154–17162 (2005).
- Coussen, F. *et al.* Recruitment of the kainate receptor subunit glutamate receptor 6 by cadherin/catenin complexes. *J. Neurosci.* **22**, 6426–6436 (2002).
- Valnegri, P. *et al.* A circadian clock in hippocampus is regulated by interaction between oligophrenin-1 and Rev-erbα. *Nat. Neurosci.* **14**, 1293–1301 (2011).

39. Ma-Högemeier, Z. L. *et al.* Oligomerization in the endoplasmic reticulum and intracellular trafficking of kainate receptors are subunit-dependent but not editing-dependent. *J. Neurochem.* **113**, 1403–1415 (2010).
40. Bassani, S. *et al.* The X-linked intellectual disability protein TSPAN7 regulates excitatory synapse development and AMPAR trafficking. *Neuron* **73**, 1143–1158 (2012).

Acknowledgements

This work was supported by Italian Ministry of Health (grant GR-2010-2318394 to J.S.) and Cariplo Foundation (2012-0593 to J.S.). We thank S.F. Heinemann (The Salk Institute for Biological Studies) and F. Laezza (Washington University School of Medicine) for providing untagged GluK2 constructs, M.D. Ehlers (Duke University Medical Center) for providing the rat-specific sh-parkin construct and the bicistronic GFP-parkin plasmid, M. Holmann (Ruhr University Bochum) for the GluK2-YFP plasmid and J. Feng (State University of New York at Buffalo) for plasmids encoding parkin domains.

Author contributions

J.S. initiated the project and performed the parkin-GluK2 interaction experiments, which were further characterized by A.M. A.M. did the western blottings on human brain samples, the *in vivo* ubiquitination analysis and the biotinylation assay. A.M. performed the pull-down assay, the *in vitro* ubiquitination assay, the excitotoxicity experiments and mouse genotyping. A.F. conducted the fluorescence imaging experiments, prepared the lentiviral particles and performed neuron infections under the direction of M.P. F.S. performed the ubiquitination assay in HEK293T cells. G.R. conducted the FRET

experiments under the direction of E.C. G.C. managed the Q311X mouse colony. Clinical samples and patient data were obtained by S.S. and N.H. M.M. performed the electrophysiology experiments. C.M. provided Myc-GluK2 plasmids, provided GluK2^{-/-} lysates and critically revised the manuscript. J.S. and A.C. conceived the study. A.M., A.C., M.P. and J.S. wrote the manuscript. All authors discussed the results, conceived further experiments, commented on the manuscript and approved the final submitted version.

Additional information

Supplementary Information accompanies this paper at <http://www.nature.com/naturecommunications>

Competing financial interests: The authors declare no competing financial interests.

Reprints and permission information is available online at <http://npg.nature.com/reprintsandpermissions/>

How to cite this article: Maraschi, A. M. *et al.* Parkin regulates kainate receptors by interacting with the GluK2 subunit. *Nat. Commun.* 5:5182 doi: 10.1038/ncomms6182 (2014).



This work is licensed under a Creative Commons Attribution 4.0 International License. The images or other third party material in this article are included in the article's Creative Commons license, unless indicated otherwise in the credit line; if the material is not included under the Creative Commons license, users will need to obtain permission from the license holder to reproduce the material. To view a copy of this license, visit <http://creativecommons.org/licenses/by/4.0/>